

Supplementary Material (ESI) for Chemical Communications  
This journal is © The Royal Society of Chemistry 2005

**Supplementary information for**

**A simple extrusion method for the synthesis of aligned silica nanowires  
using the template of a rigid surfactant mesophase**

Limin Liu, Grace Tan, Vivek Agarwal, Arijit Bose, Jibao He,  
Gary L. McPherson and Vijay T. John\*

## 1. Small Angle Neutron Scattering (SANS) Characterization of the alignment effect

SANS measurements were carried out at the National Institute of Standards and Technology (NIST) in Gaithersburg, MD, on the 30m NG3 beamline at the NIST Center for Neutron Research (NCNR). The SANS intensity,  $I(q)$ , was recorded on a 2 D detector as a function of the magnitude of the scattering vector  $q = 4\pi\sin(\theta/2)/\lambda$  where  $\theta$  is the scattering angle and  $\lambda$  is the neutron wavelength. The neutron wavelength ( $\lambda$ ) was 6 Å with a spread of 0.147 Å. Circular pinhole collimation was used. The machine was equipped with a 64cm x 64cm detector with a resolution of 1 cm<sup>2</sup>. The detector angle was set at 0° and the sample-to-detector distance was set to 4 m. The beam diameter was kept at 1.27 cm. The range of the scattering vector  $q$  for these settings was 0.0057 to 0.118 Å<sup>-1</sup>.

A mixture of D<sub>2</sub>O and distilled water at a volume ratio of 1:1 was used to form the surfactant mesophase to provide sufficient scattering contrast. Samples were contained in closed stainless steel cells with quartz windows that provided a path length of 2mm. To investigate the alignment effect from extrusion, the sample was loaded into a sample cell by first extruding it in a specific direction onto the inside surface of a quartz window and then enclosing the extrudates with another quartz window. The SANS data were corrected for empty cell scattering, detector sensitivity, background, the transmission of each sample, and were then placed on an absolute scale.

Figure 1 below shows the SANS spectra for the TMOS doped surfactant mesophase and the extruded TMOS doped surfactant mesophase at a  $W_0$  of 90. Both spectra show a strong primary peak at  $q_m = 0.040 \text{ \AA}^{-1}$  and a weak higher-order peak at  $q_{ho} = 0.069 \text{ \AA}^{-1}$ . The value of  $q_{ho}$  is  $\sqrt{3} q_m$ . Clearly, both samples show similar hexagonal

scattering patterns. Neither TMOS doping nor the extrusion process resulted in phase transition in the concentration range investigated.

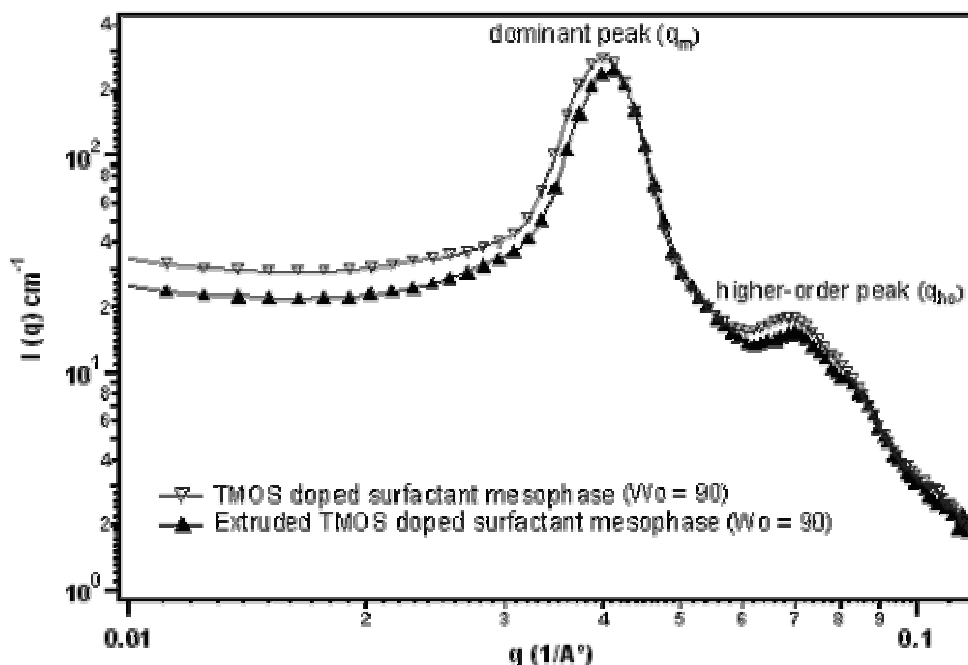
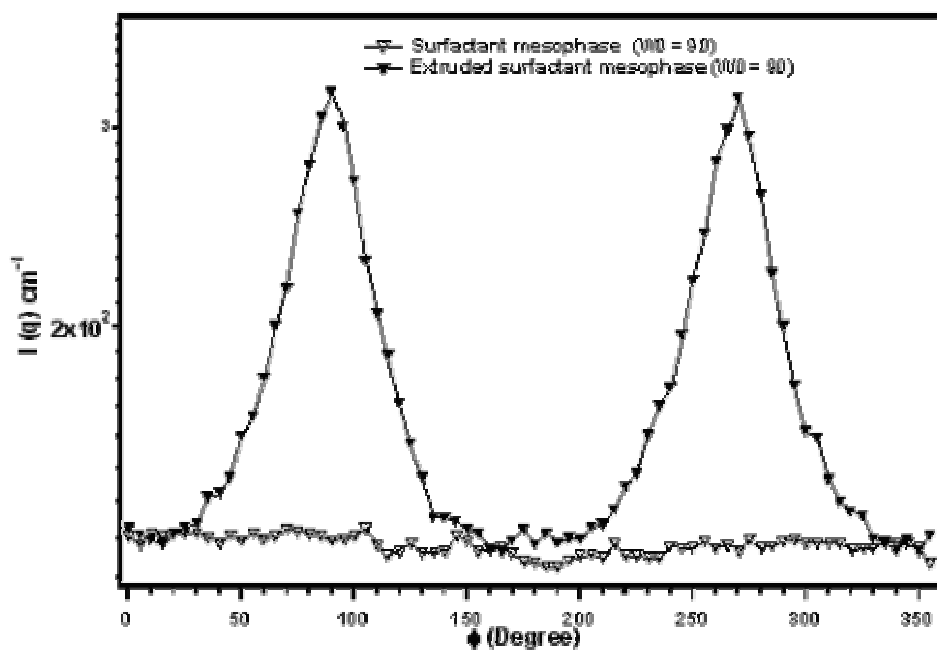


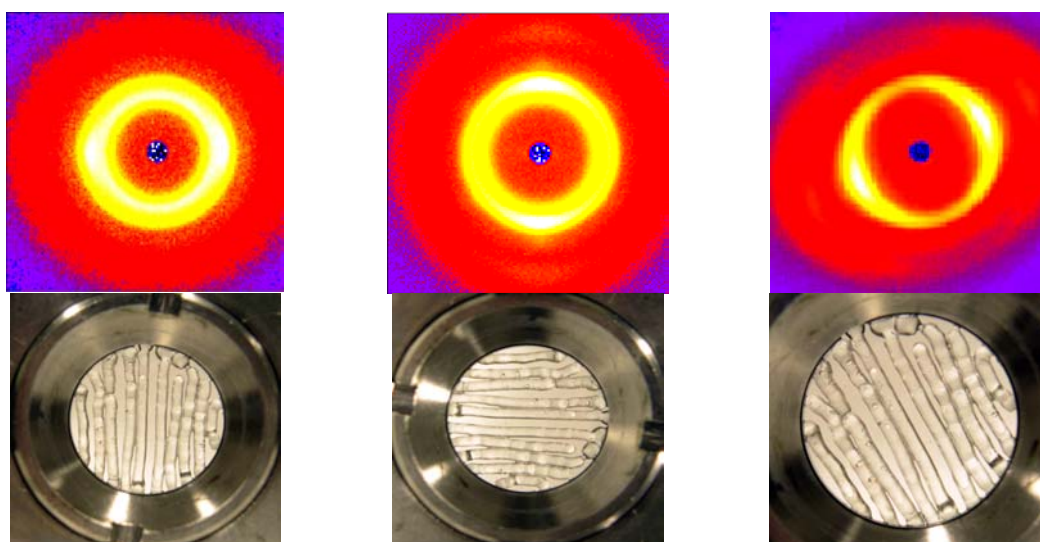
**Figure 1.** Log-log plot of the SANS data for the native TMOS doped gel and the extruded TMOS doped gel at  $W_0$  of 90. ( $W_0 = [\text{H}_2\text{O}]/[\text{AOT}]$ )

The scattering data can be further analyzed by examining the annular averaged intensity profiles at the primary peak position ( $q_m=0.04 \text{ Å}^{-1}$ ) as a function of the azimuthal angle  $\varphi$ , as illustrated in Figure 2a. No obvious orientation is observed in the native surfactant mesophase that did not undergo extrusion. In contrast, significant orientation in the direction of extrusion is clearly observed for the extruded surfactant mesophase. The 2D SANS profiles in Figure 2b shows alignment observed at different angles for samples extruded in different directions. We did not observe any breakdown in alignment 4hrs after application of extrusion. The observation indicates that the reverse

hexagonal surfactant mesophase can be easily aligned along the extrusion direction and the relaxation parameter is quite large in magnitude.



(a)



(b)

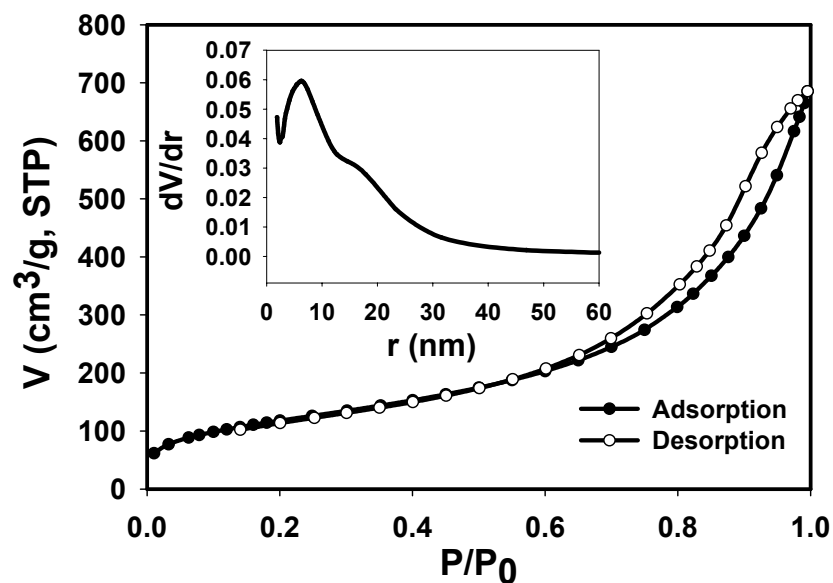
**Figure 2.** (a) An azimuthal variation of intensity at the primary peak position ( $q_m=0.04 \text{ \AA}^{-1}$ ) for the native surfactant mesophase and the extruded surfactant mesophase (extruded

tangentially to the beam line). (b) 2D SANS profiles and digital images of the samples extruded in different directions.

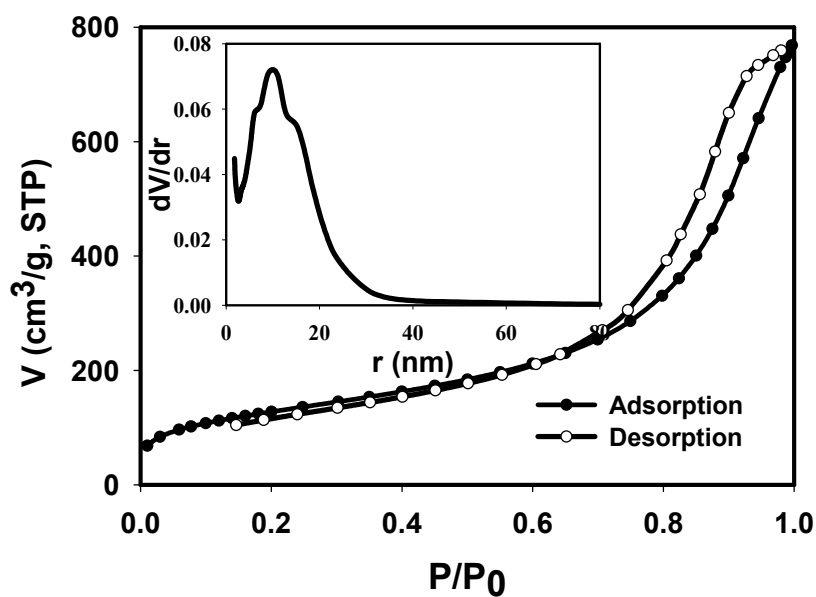
## 2. BET Surface Analysis.

The nitrogen adsorption/desorption isotherm for calcined silica synthesized from the un-extruded AOT/Lecithin mesophase is shown in Figure 3a. There is evidence of Type-IV behavior with an inflection point around  $P/P_0$  of 0.3 indicating the onset of capillary condensation. The total pore volume calculated from the adsorbed nitrogen amount at relative pressure close to the saturation vapor pressure ( $P/P_0=0.97$ ) is  $0.95 \text{ cm}^3/\text{g}$ . The silica exhibits a BET specific surface area of about  $433 \text{ m}^2/\text{g}$ . A broad pore size distribution was observed (see the inset Horvath-Kawazoe plot in Figure 3a). The evaluation of the desorption data using the Barrett-Joyner-Halenda (BJH) formula gives an average pore diameter of 8.8 nm.

The silica synthesized from the extruded AOT/Lecithin mesophase exhibits a similar Type-IV nitrogen adsorption/desorption isotherm, as shown in Figure 3b, with a broad pore size distribution (inset to Figure 3b). The total adsorption pore volume at a  $P/P_0$  of 0.97 is  $1.12 \text{ cm}^3/\text{g}$ . The calculated BET surface area is  $465 \text{ m}^2/\text{g}$ . The BJH desorption average pore size is 9.1 nm.



(a)



(b)

**Figure 3.** Nitrogen BET adsorption-desorption isotherms of (a) silica synthesized in the native AOT/Lecithin/Isooctane/Water mesophase; (b) silica synthesized in the extruded mesophase. The insets are the pore size distributions obtained from the desorption data.  $P$  is the equilibrium pressure of the adsorbate and  $P_0$  is the saturation pressure of the adsorbate at the temperature of the adsorbent.  $dV/dr$  is the derivative of the nitrogen volume adsorbed with respect to the pore diameter  $r$  of the adsorbent.